

# First-Principles Combinatorial Design of Transition Temperatures in Multicomponent Systems: The Case of Mn in GaAs

A. Franceschetti, S. V. Dudiy, S. V. Barabash, and A. Zunger\*  
National Renewable Energy Laboratory, Golden, Colorado 80401, USA

J. Xu and M. van Schilfhaarde

Department of Chemical and Materials Engineering, Arizona State University, Tempe, Arizona 85287, USA  
(Received 2 May 2006; published 27 July 2006)

The transition temperature  $T_C$  of multicomponent systems—ferromagnetic, superconducting, or ferroelectric—depends strongly on the atomic arrangement, but an exhaustive search of all configurations for those that optimize  $T_C$  is difficult, due to the astronomically large number of possibilities. Here we address this problem by parametrizing the  $T_C$  of a set of  $\sim 50$  input configurations, calculated from first principles, in terms of configuration variables (“cluster expansion”). Once established, this expansion allows us to search almost effortlessly the transition temperature of arbitrary configurations. We apply this approach to search for the configuration of Mn dopants in GaAs having the highest ferromagnetic Curie temperature. Our general approach of cluster expanding physical properties opens the way to design based on exploring a large space of configurations.

DOI: 10.1103/PhysRevLett.97.047202

PACS numbers: 75.50.Pp, 71.15.-m, 75.30.Kz, 81.05.Ea

The transition temperature  $T_C$  separating phases of different microscopic lattice order—whether configurational order/disorder in alloys [1], or ferromagnetic/paramagnetic spin ordering in magnets [2], or dipolar order/disorder in ferroelectrics [3]—constitutes an important material constant of the solids exhibiting these phenomena. The quest for materials with desired  $T_C$ 's, such as high-temperature superconductors or room-temperature ferromagnetic semiconductors, characterizes much of contemporary materials science. The ability to intentionally grow in the laboratory different structural realizations of substitutional alloys, even in defiance of thermodynamical equilibrium, has opened up the challenging prospect of attaining special  $T_C$ 's by manipulating the growth parameters. Indeed, the realization that transition temperatures can be controlled by alloying two or more component materials has spurred considerable interest in materials engineering of metal alloys [1], multicomponent superconducting alloys [4], ferromagnetic semiconductor alloys made of both magnetic and nonmagnetic components [2], ferroelectric alloys [3], etc. Interestingly, the transition temperature of the combined, multicomponent system rarely follows a constituent-average, linear behavior. Instead,  $T_C$  is often determined by the *microscopic atomic arrangement* in the system. Numerous attempts [5,6] have already been made to grow  $\text{Ga}_{1-x}\text{Mn}_x\text{As}/\text{GaAs}$  heterostructures, “digital alloys,” and superlattices in a yet unguided, empirical quest for a configuration with high  $T_C$ . However, the combinatorial explosion of the number of configurational possibilities ( $2^N$  for a binary system on  $N$  lattice sites) is such that trial-and-error approaches can be successful only by virtue of lucky accidents.

At the same time, solid state theory has progressed to a point where  $T_C$  of ferromagnets [7,8] and ferroelectrics [9] (but not as yet superconductors) can be predicted semi-

quantitatively even in structurally complex compounds. However, the same combinatorial explosion that has plagued experimental explorations hinders theoretical searches of configurations with desired  $T_C$ , for even though one can calculate  $T_C$  of a few configurations, it is impractical to compute  $\sim 2^N$  values of  $T_C$ . We suggest here a general solution to this dilemma whereby time-consuming but accurate first-principles calculations of  $T_C$  of a few ordered configurations are parametrized via an expansion in configuration variables, permitting afterwards a nearly effortless exploration of an astronomic number of configurations in search of the one with the target  $T_C$ . We illustrate this method using the Curie temperature of Mn-doped GaAs as an example. This approach opens the way to the deliberate design of transition temperatures in a broad range of materials science problems.

We use the cluster-expansion formalism [10] to parametrize a generic material property  $P$ , e.g., the Curie temperature. Each of the  $2^N$  lattice configurations  $\{\sigma\}$  of a binary system is defined by the occupation pattern  $\{S_1, \dots, S_N\}$  of the  $N$  lattice sites by either an  $A$  atom ( $S_i = -1$ ) or a  $B$  atom ( $S_i = 1$ ). The physical property  $P$  can then be cluster expanded in terms of geometric objects such as pairs, triangles, etc.:

$$NP(\sigma) = \sum_i \tau_i S_i + \sum_{i,j} \tau_{i,j} S_i S_j + \sum_{i,j,k} \tau_{i,j,k} S_i S_j S_k + \dots, \quad (1)$$

where  $\tau_i$ ,  $\tau_{i,j}$ ,  $\tau_{i,j,k}$ , etc., are expansion coefficients (independent of  $\sigma$ ), and the expansion is mathematically exact [11] if all  $2^N$  coefficients are retained. Once established, this expansion permits a nearly effortless exploration of a very large number of configurations in search of the one with the target value for the property  $P$ .

Our procedure involves three steps (i)–(iii), which we describe in what follows:

(i) *Calculating the transition temperature of given atomic configurations.*—To calculate the Curie temperature of Mn-doped GaAs we use the Heisenberg Hamiltonian  $H = -\sum_{i,j} J_{ij}(\sigma) s_i \cdot s_j$ , where each Mn-occupied site  $i$  in the atomic configuration  $\sigma$  has a (generally noncollinear) spin moment  $s_i$ , and  $\{J_{ij}(\sigma)\}$  are the Mn-Mn pair exchange energies for the atomic configuration  $\sigma$ . The exchange energies are calculated here from linear-response theory (LRT) [12], based on the local-density approximation (LDA) to density-functional theory. The LRT assumes the rigid-spin and long-wavelength approximations [13], which are satisfied in the low Mn concentration range where the magnetic moments are large ( $\mu \sim 4\mu_B$ ) and localized on the Mn atoms. We use the LRT implementation of van Schilfgaarde and Antropov [14], based on the linear muffin-tin orbital atomic-sphere approximation approach. Once we have obtained  $\{J_{ij}(\sigma)\}$  for a given configuration  $\sigma$ , we calculate  $T_C(\sigma)$  from a Monte Carlo simulation of the Heisenberg Hamiltonian. We use a simulation cell of up to  $8 \times 8 \times 8$  or  $10 \times 10 \times 10$  times the unit cell used to calculate  $\{J_{ij}(\sigma)\}$ . Long-range exchange pair interactions extend up to  $\sim 15$  neighbors (see Fig. 1) and are fully included in the Monte Carlo simulation. The number of Monte Carlo steps ( $\sim 10^4$ – $10^5$ ) and the number of independent Monte Carlo runs are systematically increased until the statistical error bars of the cumulants [15] allow us to determine  $T_C$  to within  $\sim 3$  K. Our methodology differs from, and improves on, a number of approximations proposed in the literature [16–22]:

(a) *Exchange energies are determined by small-angle rotations:* The LRT provides the exchange energies appropriate to *small-angle* spin rotations, as required by the Heisenberg representation, thus avoiding the approximation [16] of obtaining  $J_{i,j}$ 's from purely ferromagnetic and purely antiferromagnetic *large-angle* spin rotations.

(b) *The CPA is avoided:* In our approach, each cation lattice site  $i$  in the supercell is occupied by either a Mn or a Ga atom. This automatically creates many different local environments for the Mn ions. In the coherent potential approximation (CPA) [17], each Mn ion experiences instead the same potential and the same magnetic moment, irrespective of its environment. The importance of such “environmental effects” [18] is apparent from Fig. 1(a), which shows that for a given crystal structure (in this case a  $\text{Ga}_{92}\text{Mn}_8\text{As}_{100}$  supercell) there are different values of  $J_{i,j}$  for pairs of atoms separated by the same distance, but having different atomic environments (plurality effect). The CPA misses the existence of such distribution in ordered structures and random alloys (in the latter case, environmental effects are diminished but do not average out [19]).

(c) *The pair-superposition approximation is avoided:* We determine the magnitude of  $J_{i,j}(\sigma)$  for each  $(i, j)$  pair in the presence of other “spectator” Mn atoms, thus avoiding the superposition approximation [20], where  $J_{i,j}$  for pair  $(i, j)$  is determined from a supercell calculation including Mn atoms only at sites  $i$  and  $j$ . The importance of such nonsuperposition effects is apparent from a comparison of Figs. 1(a) and 1(b). In Fig. 1(a), the Mn-Mn exchange interactions  $J_{i,j}$  were calculated in the presence of spectator Mn atoms in the supercell. In Fig. 1(b), the Mn-Mn exchange interactions were obtained from *isolated* Mn-Mn pairs. Figures 1(a) and 1(b) demonstrate that the exchange energies depend on the atomic configuration.

(d) *The mean-field approximation to  $T_C$  is avoided:* We obtain the Curie temperature from Monte Carlo simulations of the Heisenberg Hamiltonian. We find that the mean-field approximation [21] systematically overestimates  $T_C$ , and the error can be as large as 50%. A similar conclusion was arrived at by Sato *et al.* [22].

In general, we find  $J_{i,j}(\sigma)$  to be nonmonotonic as a function of the  $i$ - $j$  distance, to exhibit the “plurality effect” and to extend up to  $\sim 15$  nearest-neighbor shells [Fig. 1(a)]. For a substitutional random alloy ( $x_{\text{Mn}} = 8\%$ ) our procedure yields  $T_C = 230$  K, this being an upper bound to the currently measured value  $T_C \approx 160$  K [23] for a nearly uncompensated (Ga,Mn)As alloy. Clustering effects present in currently grown samples might explain [7,24] the lower than ideal  $T_C$ .

(ii) *Establishing a cluster expansion from a set of directly calculated  $\{T_C(\sigma)\}$ .*—This is done using the iterative procedure described in Ref. [25] in the context of cluster expansion of formation energies. We start by calculating  $\{T_C^{\text{LDA}}(\sigma_{\text{input}})\}$  of a set of input structures  $\{\sigma_{\text{input}}\}$ , consisting of all periodic structures comprised of one Mn atom and up to five Ga atoms in the unit cell. These input

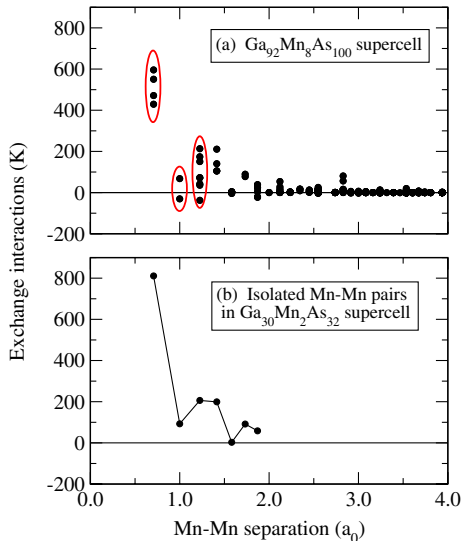


FIG. 1 (color online). The exchange interaction between pairs of Mn atoms, calculated in the linear-response approximation, is shown as a function of the Mn-Mn distance for (a) a  $\text{Ga}_{92}\text{Mn}_8\text{As}_{100}$  supercell containing 6 Mn spectator atoms in addition to the Mn pair, and (b) a set of isolated Mn-Mn pairs in a  $\text{Ga}_{30}\text{Mn}_2\text{As}_{32}$  supercell. Red circles indicate pairs of Mn atoms that are separated by the same distance, but have different  $J_{ij}$ 's because of the presence of spectator Mn atoms.

structures represent a range of Mn concentrations and layer orientations. We then use the calculated  $\{T_C^{\text{LDA}}(\sigma_{\text{input}})\}$  to determine the coefficients of Eq. (1). We include in the expansion of Eq. (1) all two-body interactions up to the 24th nearest-neighbor shell in the fcc sublattice, and several (6–8) many-body interaction types (MBITs), selected using the genetic-algorithm (GA) approach [25]. We then evaluate via Eq. (1)  $T_C$  of many other structures not included in the input set. Some of these structures are found to have higher  $T_C$  than those included in the input set. Therefore, in the next cluster expansion (CE) iteration, we calculate  $T_C^{\text{LDA}}(\sigma)$  of those new high- $T_C$  structures [using the method described in (i) above], add them to the previous input set, and repeat the GA selection of MBITs. The iterations are repeated until no new structures with higher  $T_C$  are predicted (typically 4–5 iterations are sufficient). The final MBITs are shown graphically in Fig. 2(a). To test the quality of the cluster expansion we finally apply it to complex structures, never used in the fitting procedure, and compare  $T_C$  calculated from the cluster expansion ( $T_C^{\text{CE}}$ ) with  $T_C$  calculated directly from LDA-LRT ( $T_C^{\text{LDA}}$ ). For a random  $\text{Ga}_{92}\text{Mn}_8\text{As}_{100}$  alloy ( $x_{\text{Mn}} = 8\%$ ) we find  $T_C^{\text{CE}} = 234$  K and  $T_C^{\text{LDA}} = 230$  K, while for a  $\text{Ga}_{56}\text{Mn}_8\text{As}_{64}$  alloy ( $x_{\text{Mn}} = 12.5\%$ ) we obtain  $T_C^{\text{CE}} = 267$  K and  $T_C^{\text{LDA}} = 265$  K. These configurations represent the limit of complexity that can now be calculated directly by first principles, yet the cluster-expansion estimate for them is obtained effortlessly ( $<1$  s).

(iii) *Searching for special configurations.*—The expansion of Eq. (1) can now be readily applied to predict the Curie temperature  $T_C$  of a very large number of atomic configurations. This is illustrated in Fig. 2(b), which shows  $T_C$  for  $\sim 2^{20}$  ordered structures as a function of the Mn concentration  $x_{\text{Mn}}$ . We include in the search all periodic structures consisting of up to 20 cations (Ga or Mn) in the unit cell, including all possible substitutional arrangements (random, clusters of impurities, superlattices, ordered compounds). We do not display results for the high Mn-concentration range, a composition regime that is not represented well by the linear-response theory [26]. We find that for many compositions the highest  $T_C$  structures are  $(\text{GaAs})_m/(\text{MnAs})_n$  superlattices in the (201) orientation. For example, the highest- $T_C$  structure for  $x_{\text{Mn}} = 33\%$  is a  $(\text{GaAs})_2/(\text{MnAs})_1$  (201) superlattice. For comparison, Fig. 2(b) also shows the  $T_C$  of a random alloy [calculated by performing analytically a configuration average over Eq. (1)] as a function of Mn concentration (solid line). We see from Fig. 2(b) that many ordered structures are predicted to have  $T_C$ 's 100 K or more above the random alloy, suggesting that structural details are important and that above room temperature  $T_C$ 's can be achieved by growing GaAs/MnAs ordered superlattices. For example, the  $(\text{GaAs})_2/(\text{MnAs})_1$  (201) superlattice has a predicted  $T_C$  of 355 K, compared with  $T_C = 160$  K for a random alloy of the same composition. The emergence of ordered (201) superlattices as the highest  $T_C$  ferromagnets in this family

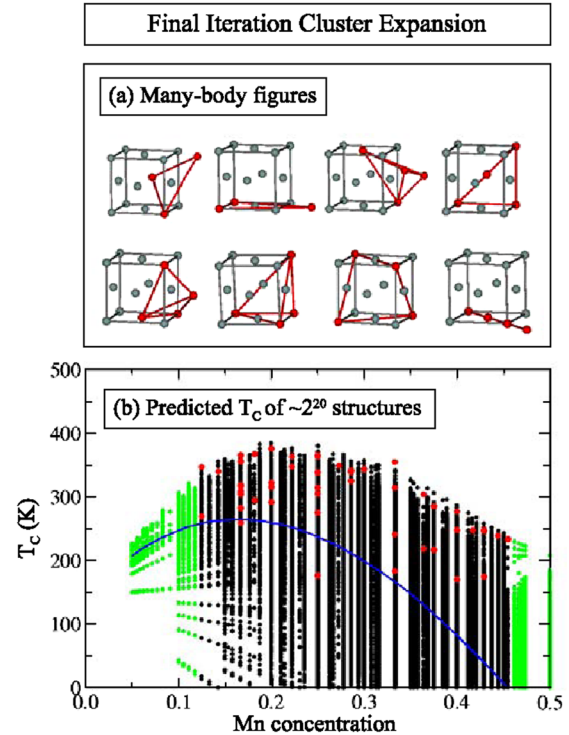


FIG. 2 (color online). Final iteration cluster expansion. Part (a) shows the many-body figures obtained from the genetic-algorithm search. Part (b) shows the predicted  $T_C$  of  $\sim 2^{20}$  ordered structures. The black circles indicate structures that fall inside the composition range used for the cluster expansion ( $0.12 < x < 0.46$ ), while green or light gray circles denote structures outside that range. Red or medium gray circles denote the input structures that were used in the fit of the cluster-expansion coefficients. The solid blue line shows the predicted  $T_C$  of a random alloy as a function of Mn concentration.

is rather unsuspected. We find that these structures are characterized by strong ferromagnetic coupling between adjacent Mn planes, induced by Mn-Mn interactions along the (110) direction. Previous first-principles calculations [20] had shown that the magnetic interaction between two Mn atoms is stronger if the pair is oriented along the (110) direction. For other superlattice orientations, such as (100) or (111), no such strong interactions between Mn planes exist, thus explaining the lower  $T_C$ .

To provide theoretical guidance and physical insight to the growth of high- $T_C$  structures, we have applied our CE to predict  $T_C$  of various “digital superlattices” in orientations that can be grown experimentally. The  $T_C$  of pure  $(\text{GaAs})_m/(\text{MnAs})_1$  superlattices in several crystallographic orientations is shown in Fig. 3(a). Interestingly, (201) is the only orientation for which  $T_C$  does not decrease monotonically as the interlayer spacing  $m$  increases. Instead,  $T_C$  has a maximum ( $\sim 375$  K) for  $m = 4$ , corresponding to  $x_{\text{Mn}} = 20\%$ . Other orientations that have large  $T_C$  ( $>250$  K) are (311) and (110). All these superlattice orientations have Curie temperatures above the random alloy (for  $x_{\text{Mn}} > 0.13$ ), suggesting that the Curie tempera-

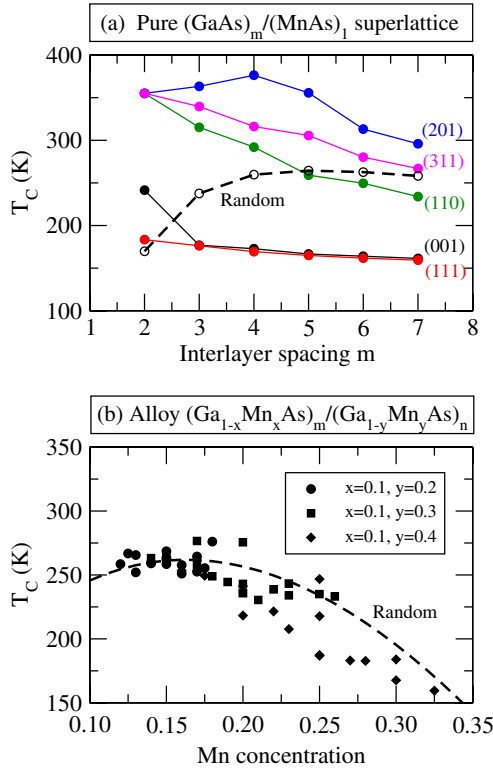


FIG. 3 (color online). (a) Predicted  $T_C$  of several  $(\text{GaAs})_m/(\text{MnAs})_n$  pure superlattices in different crystallographic orientations. Also shown is the  $T_C$  of the random alloy (black dashed line). (b) Predicted  $T_C$  of  $(\text{Ga}_{1-x}\text{Mn}_x\text{As})_m/(\text{Ga}_{1-y}\text{Mn}_y\text{As})_n$  alloy superlattices in the (001) orientation. For each set of layer compositions  $(x, y)$ , the layer thicknesses  $(m, n)$  are allowed to vary between 1 and 4. The dashed line denotes the  $T_C$  of the random alloy.

ture of the random alloy can be exceeded by growing digital heterostructures on currently unsuspected substrate orientations. Since it is often easier to grow *alloy* superlattices, we show in Fig. 3(b) results for  $(\text{Ga}_{1-x}\text{Mn}_x\text{As})_m/(\text{Ga}_{1-y}\text{Mn}_y\text{As})_n$  (001) superlattices where each cation layer consists of a random distribution of Ga and Mn atoms. We see from Fig. 3(b) that although the resulting  $T_C$  does not deviate too much from the random alloy of identical composition, several superlattice structures have  $T_C$  that exceeds that of the random alloy. This is the case, for example, of the  $(\text{Ga}_{0.9}\text{Mn}_{0.1}\text{As})_2/(\text{Ga}_{0.7}\text{Mn}_{0.3}\text{As})_1$  alloy superlattices, which we find to have a  $T_C$  of  $\sim 275$  K. This result suggests that the Curie temperature can be increased by growing specific sequences of (Ga,Mn)As alloy layers.

In conclusion, we have shown that the cluster-expansion formalism, originally formulated to parametrize the formation energies of substitutional alloys, can be generalized to predict the *transition temperatures* of multicomponent systems. We have applied this method to calculate the Curie temperature of many different configurations of the (Ga,Mn)As alloy. We find that the highest  $T_C$  ( $> 350$  K) is achieved for  $(\text{GaAs})_m/(\text{MnAs})_n$  superlattices in the (201)

orientation. Our results open the way to the design of ordered alloys with desired transition temperatures.

This work was supported by DARPA, Defense Sciences Office, under NREL Contract No. DEAC36-98-GO10337. J.S. and M.v.S. were supported by ONR Contract No. N00014-02-1-1025.

\*Electronic address: alex\_zunger@nrel.gov

- [1] A. B. Chen and A. Sher, *Semiconductor Alloys: Physics and Materials Engineering* (Kluwer, New York, 1995).
- [2] D. C. Mattis, *The Theory of Magnetism: Statics and Dynamics* (Springer, New York, 1988).
- [3] *Fundamental Physics of Ferroelectrics 2002*, edited by R. E. Cohen (Springer, New York, 2002).
- [4] J. C. Phillips, *Physics of High- $T_C$  Superconductors* (Elsevier, New York, 1989).
- [5] R. K. Kawakami *et al.*, Appl. Phys. Lett. **77**, 2379 (2000).
- [6] G. Kioseoglou *et al.*, Appl. Phys. Lett. **80**, 1150 (2002).
- [7] J. L. Xu, M. van Schilfhaarde, and G. D. Samolyuk, Phys. Rev. Lett. **94**, 097201 (2005).
- [8] G. Bouzerar *et al.*, Phys. Rev. B **68**, 081203 (2003).
- [9] L. Bellaiche, A. Garcia, and D. Vanderbilt, Phys. Rev. Lett. **84**, 5427 (2000).
- [10] A. Zunger, in *Statics and Dynamics of Alloy Phase Transformations*, NATO ASI (Plenum Press, New York, 1994), p. 361.
- [11] J. M. Sanchez, F. Ducastelle, and D. Gratias, Physica (Amsterdam) **128A**, 334 (1984).
- [12] A. I. Lichtenstein *et al.*, J. Magn. Magn. Mater. **67**, 65 (1987).
- [13] V. P. Antropov, J. Magn. Magn. Mater. **262**, L192 (2003).
- [14] M. van Schilfhaarde and V. P. Antropov, J. Appl. Phys. **85**, 4827 (1999).
- [15] D. P. Landau and K. Binder, *A Guide to Monte Carlo Simulations in Statistical Physics* (Cambridge University Press, Cambridge, 2000).
- [16] A. J. R. da Silva *et al.*, J. Phys. Condens. Matter **16**, 8243 (2004).
- [17] K. Sato *et al.*, J. Phys. Condens. Matter **16**, S5491 (2004).
- [18] R. Magri, S. H. Wei, and A. Zunger, Phys. Rev. B **42**, 11388 (1990).
- [19] Z. W. Lu, S. H. Wei, and A. Zunger, Phys. Rev. B **44**, 10470 (1991).
- [20] P. Mahadevan, A. Zunger, and D. D. Sarma, Phys. Rev. Lett. **93**, 177201 (2004).
- [21] K. Sato, P. H. Dederichs, and H. Katayama-Yoshida, Europhys. Lett. **61**, 403 (2003).
- [22] K. Sato *et al.*, Phys. Rev. B **70**, 201202 (2004).
- [23] F. Matsukura, H. Ohno, and Y. Sugawara, Phys. Rev. B **57**, R2037 (1998).
- [24] K. Sato, H. Katayama-Yoshida, and P. H. Dederichs, Jpn. J. Appl. Phys. **44**, L948 (2005).
- [25] G. L. W. Hart *et al.*, Nat. Mater. **4**, 391 (2005).
- [26] For zinc-blende MnAs we find  $\delta E_{\text{LDA}} = E_{\text{FM}} - E_{\text{AFM}} = -33$  meV/Mn, whereas calculating the same quantity from LRT gives  $\delta E_{\text{LRT}} = 122$  meV/Mn. For a  $(\text{GaAs})_2/(\text{MnAs})_2$  superlattice in the (201) orientation (chalcopyrite structure), we find  $\delta E_{\text{LDA}} = -147$  meV/Mn and  $\delta E_{\text{LRT}} = 29$  meV/Mn.